**IAES International Journal of Artificial Intelligence (IJ-AI)**
Vol. 12, No. 3, September 2023, pp. 1329~1341
ISSN: 2252-8938, DOI: 10.11591/ijai.v12.i3.pp1329-1341 

# Facial recognition using multi edge detection and distance measure

**Indo Intan[1], Nurdin[1], Fitriaty Pangerang[2]**
[1]Department of Informatics Engineering, Universitas Dipa Makassar, Makassar, Indonesia
[2]Department of Electronics Engineering, Polytechnic Negeri Ujung Pandang, Makassar, Indonesia

**Article Info**

***Article history:***

Received Dec 24, 2021
Revised Apr 26, 2022
Accepted May 19, 2022

***Keywords:***

Canberra distance
Combination edge detection
Distance measure
Edge detection
Face recognition

**ABSTRACT**

Face recognition provides broad access to several public devices, so it is essential in cutting-edge technology. Human face recognizing has challenge in using uncomplicated and straightforward algorithms quickly, using memory specifications are not too high, otherwise the results are quality and accurate. Face recognition using combination edge detection and Canberra distance can be recommended for applications that require fast and precise access. The application of several edge detections singly has low performance, so it requires a combination technique to obtain better results. The proposed method combined several edge detections such are Robert, Prewitt, Sobel, and Canny to recognize a face image by identification and verification. As a feature extractor, the combination edge detection forms a more robust and more specific facial pattern on the contour lines. The results show that the combination accuracy outperforms other extractor features significantly. Canberra distance produces the best performance compared to Euclidean distance and Mahalanobis distance.



***Corresponding Author:***

Indo Intan
Department of Informatics Engineering, Universitas Dipa Makassar
Jl. Perintis Kemerdekaan KM. 09, Talamanrea, Makassar, Indonesia
Email: indo.intan@undipa.ac.id

## 1. INTRODUCTION

A valid identification and verification process need face detection and recognition are essential. Facial biometrics have the exact resemblance from one person to another even though they have faces that are not twins or identical, but the error calculation is still often high. The solution is based on previous research, namely, highly accurate feature extraction and classification processes. Face recognition systems have been widely implemented in various accesses, making it easier for humans to carry out their activities. The challenge for face detection is to detect faces quickly and efficiently using a simple, too-complex algorithm to obtain good quality and effective solutions [1]. Edge detection is one of the techniques used in the feature extraction section, as the first step that aims to retrieve information from the image [2].

The previous researchers have carried out various approaches and techniques, including several previous studies on edge detection, including edge detection through a single Sobel technique [3]; Canny technique [4]. Likewise, research on the fusion or merging of several feature extractions of Sobel and Canny [5], [6]; Sobel and Gaussian [7]; edge detection fusion and combination of Sobel, support vector machine (SVM), and convolutional neural network (CNN) [8]; Canny and Prewitt [9]; Sobel, Prewitt, Roberts, Canny, Laplacian of Gaussian (LoG), expectation-maximization (EM), Otsu, and genetics [10]. They have obtained include complementing the shortcomings of every single method to produce a better image; better accuracy, so that information retrieval is valid [2]; can overcome noise in the image due to the presence of fine threshold wavelet de-noising [7]; able to provide memory operation performance by reducing memory usage by 40% and processor operation by 50% in reading logic of field programmable gate array (FPGA) architecture [3]; classifying facial expressions, which increased system recognition by 3.71% after the addition of Sobel; produce better input segmentation [9]; the use of faster computing time because the image resolution used is low so the results are significant [5]; and the segmentation results are more stable [10].

The basic steps to develop a robust face recognition system [11] are: i) the face detection as the first step to localize the human faces in a particular image. Its purpose is to determine human face or not; and ii) feature extraction as the next step if the human face is detected to extract the features of the face images segmented. This step represents a face as features vector called a signature. It describes the face segmented such as mouth, nose, and eyes with their geometry distribution [11], [12]; iii) face recognition as the last step to consider the feature extracted and compares it faces image stored in a faces database (faces gallery) [11]. The other word, a face recognition is a classification process to recognize probe face as one of the number faces in the stored face gallery [13]. Previous research Table 1 has not completed the integration of edge detection in the accumulation of the pixel value of the image, only comparing singly or combining two or three edge detections. The classification method used is also more complicated in their algorithms. They used the combination algoritms too, two or more, but they had not used combining of edge detection. They had used the other feature extraction algorithms, the more complicated feature extraction. This research focuses on the optimization of edge detection through a summation of the four. It is a simple algorithm to achieve better performance.

Table 1. The approach and results of previous research

| No | Author | Feature extractor | Classifier | Result | Limitation |
|---|---|---|---|---|---|
| 1 | Intan [13] | Component dependent analysis | Euclidean distance, threshold distance | - The accuracy=96.36% | - Dataset is still less.<br>- Inrespective of various pose and rotation |
| 2 | Boyko *et al.* [14] | DLib, OpenCV Lib, HOG | SVM, deep CNN (DCNN) | Recognition time OpenCVLib <dlib | - It is still needing other feature extractors like Haar for exploration. |
| 3 | Lakshmi and Patilkulakarn i [9] | Canny and Prewitt | City block measure | - False rejection rate is improvement false acceptance rate (FAR) is lower. | - Robust classification is lower. |
| 4 | Hashim and Shalan [15] | - Hybrid between Gabor filter and singular value decomposition<br>- Image size 64x64 | The statistical measure | - The accuracy of AT&T dataset: 77.7-100%<br>- The accuracy of fan energy index (FEI):84-100% | - The statistical measure is tricky, and it has random behavior<br>- The fluctuation of changes in accuracy increase is affected by the number of training sets |
| 5 | Veni e*t al.* [16] | - Optimalization of Sobel edge detection+ACO | Matching algorithm | Precision rate=1 and error rate=0<br>- Efficient and better recognition efficiency and recall rate. | - It has limitations on rotation invariant, occluded images, head poses. |
| 6 | Faraji and Qi [17] | AdaS, Gradientface, Weberface, local binary pattern (LBP), local direction pattern (LDP), enhanced LDP (EnLDP), local directional number pattern (LDN). | Eigth local directional pattern (ELDP) | - The accuracy is 98.29% (CMU-PIE face database)<br>- The accuracy is 100% (Yale B face database) | - The sample of each subject in the training data is still lacking. |
| 7 | Ali *et al.* [18] | LBP, LBP variance (LBPV), principal component analysis (PCA), kernel discriminative common vectors (KDCV). | Neural network | - The accuracy of FG-NET face aging database: 93% | - The number of samples and the age ranges are still small. |
| 8 | Kihal *et al.* [19] | Gabor filtering, phase encoding, linear discriminant analysis (LDA) | Hamming distance measure | - False rejection rate (FRR) =% at 0.1% FAR; equal error rate (EER)=0.0916%<br>- FRR=0.18% at 0.1% FAR; EER=0.18%% | - Database limitations.<br>- No ocular feature yet. |
| 9 | Manju and Radha [20] | Histogram (HOG), weighted-LBP(WLBP), histogram of face orientation (HFO), histogram of face direction (HFD) | Orthogonal locality preserving projection (OLPP), POLPP | Spatio-temporal frequent object mining-Viola-Jones based face detection-pose invariant OLPP (STFOM-FD-PIOLPP) are better than STFOM-FD-OLPP and STOFM-FD-LPP. The significant difference is 0-52-6.8%. | - It has limitations on rotation invariant, occluded images, head poses. |

The purpose of this study is to show the significance of selecting multiple feature extractions and classifiers in face recognition so that the system performance is better than using only one or two extractors and classifiers. Does using a combination of edge detection have better accuracy than single or double edge detection? How does the distance measure compare to the classifier? Which detection outperforms the others?

## 2. PROPOSED METHOD

The method used in this research is as showed in Figure 1. These are the step of the research methods: preprocessing, feature extraction process, classification process, and recognition. The figure 1 is described on section 2.1 to 2.4.

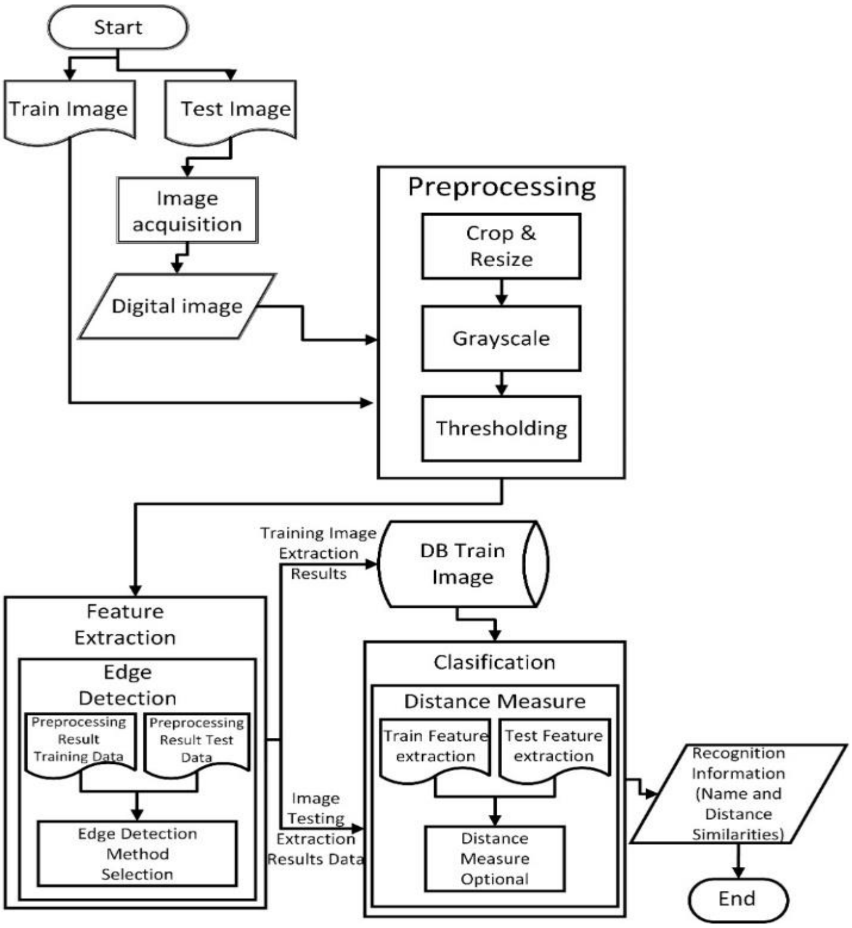


Figure 1. The flowchart of the multi edge detection and distance measure models and experimental methods applied

### 2.1. Data acquisition

This study uses 300 datasets sourced from Olivetti Research Laboratorium (ORL) and direct sampling. The source of this face sample comes from 30 respondents. Each person has ten samples, so there are 300 samples in total. The samples are divided into 270 training image samples and 30 testing face samples. Then the multi-edge detection feature extraction process is carried out to produce 5 sample classes. Each edge detection produces 270 images so that the total image samples are 5×270 samples=1,350 train image samples. The sample image is stored in the database, while the test image has 30 sample images to test system performance. All samples were taken from each person as many as ten poses with various positions, including front, left side, right side, smile, flat expression, and smiling expression.

The cropping process was carried out of the image dataset measuring 1,100×1,500 pixels to 100×100 pixels. Its small size reduced the use of computing memory. The greyscale process changed the original image to gray with a gray level of 0-255. Next, the gray image passed through the threshold process as a binary image process (Figure 1). Images cropped as frontal faces with variation in facial expressions, pose variation and illumination conditions.

## 2.2. Face extracture using multi edge detection
### 2.2.1. Robert edge detection

Chen and Cheng [21], Razzok *et al.* [22], Robert has explained that using a gradient operator with two 2×2 pixel matrices in (1). The process is to convolute grayscale images with Robert kernel matrix in horizontal (*H*) and vertical (*V*) directions, *G* is gradient pixels value; *Gx* is Robert horizontal gradient value; *Gy* is Robert vertical gradient value. It is shown in (1) [5].

$$H=\begin{bmatrix}1 & 0\\ 0 & -1\end{bmatrix} \text{ dan } V=\begin{bmatrix}0 & -1\\ 1 & 0\end{bmatrix} \tag{1}$$

Convolution is carried out as in (2) and (3)

$$G_x=\frac{\partial f(x,y)}{\partial_x}=f(x,y)-f(x-1,y) \tag{2}$$

$$G_y=\frac{\partial f(x,y)}{\partial_y}=f(x,y)-f(x,y-1 \tag{3}$$

### 2.2.2. Prewitt edge detection

Compare to Roberts results, Prewitt used 3×3 size gradient matrix in (9). The Prewitt method involves convoluting grayscale images with Its matrix in horizontal (*H*) and vertical (*V*) directions. *G* is gradient value or pixel value (x, y); *Gx* is horizontal Prewitt gradient value; *Gy* is vertical Prewitt gradient value (4) [5], [21], [22].

$$H=\begin{bmatrix}-1 & 0 & 1\\ -1 & 0 & 1\\ -1 & 0 & 1\end{bmatrix} \text{ dan } V=\begin{bmatrix}-1 & -1 & -1\\ 0 & 0 & 0\\ 1 & 1 & 1\end{bmatrix} \tag{4}$$

Matrix convolution is carried out as in (5) and (6).

$$G_x=(a_2+a_3+a_4)-(a_0+a_7+a_6) \tag{5}$$

And

$$G_y=(a_0+a_1+a_2)-(a_6+a2+a_4) \tag{6}$$

Next, the gradient magnitude is calculated using (7):

$$G=\sqrt{\left(\frac{\partial f}{\partial x}\right)^2+\left(\frac{\partial f}{\partial y}\right)^2}=\sqrt{G_x^{\ 2}+G_y^{\ 2}} \tag{7}$$

### 2.2.3. Sobel edge detection

Sobel has more improvement result than Roberts's, which uses a gradient operator, but the matrix used is 3×3 pixels, as shown in (5). The Sobel method is done by convoluting grayscale images with a Sobel matrix in *H* and *V* directions [21]. It performs a two dimensional (2-D) spatial gradient measurement on the image. Typically, it is used to find the approximate absolute gradient magnitude at each point in the input grayscale image [5]. As edge detector, it uses a pair of convolution masks, one estimating the gradient in the x-direction (columns) and the other estimating the gradient in the y-direction (rows) such as equation (10)-(12) [5].

A convolution mask is usually much smaller than the actual image. As a result, the mask is shifted over the image, manipulating a square of pixels at a time.

$$H=\begin{bmatrix}-1 & 0 & 1\\ -2 & 0 & 2\\ -1 & 0 & 1\end{bmatrix} \text{ dan } V=\begin{bmatrix}-1 & -2 & -1\\ 0 & 0 & 0\\ 1 & 2 & 1\end{bmatrix} \tag{8}$$

Pixels are converted into a matrix as in (9):

$$f(x,y)=\begin{bmatrix} a_0 & a_1 & a_2 \\ a_7 & (x,y) & a_3 \\ a_6 & a_5 & a_4 \end{bmatrix} \quad (9)$$

f(x,y) is pixel size of the image in the matrix; $a_n$ is pixel value in the matrix; (x,y) is new pixel value from the convolution. Sobel method matrix convolution is done by (10) and (11).

$$G_x=(a_2+2a_3+a_4)-(a_0+2a_7+a_6) \quad (10)$$

$$G_y=(a_0+2a_1+a_2)-(a_6+2a_5+a_4) \quad (11)$$

Next, the gradient is calculated using (12) with the *G* value is gradient value or pixel value (x,y); *Gx* is horizontal direction Sobel gradient value; *Gy* is Sobel gradient value in the vertical direction.

$$G=\sqrt{\left(\frac{\partial f}{\partial x}\right)^2+\left(\frac{\partial f}{\partial y}\right)^2}=\sqrt{G_x{}^2+G_y{}^2} \quad (12)$$

**2.2.4. Canny edge detection**

The Canny method starts from entering an image in grayscale and then performs a Gaussian filtering process with=1.4. The aim is to filtering noise from the initial image to get a smooth edge image. Furthermore, the convolution is carried out with (13).

$$\frac{1}{159}\begin{bmatrix} 2 & 4 & 5 & 4 & 2 \\ 4 & 9 & 12 & 9 & 4 \\ 5 & 12 & 15 & 12 & 5 \\ 4 & 9 & 12 & 9 & 4 \\ 2 & 4 & 5 & 4 & 2 \end{bmatrix} \quad (13)$$

The kernel above is a Gaussian kernel of order 5×5 with=1.4. Then, the magnitude of the gradient uses (14) below [5], [22]. The Canny kernel is convoluted with images, starting from the left row to the right side one pixel until it reaches the entire length horizontally. When it finished doing, the continued processing to reach the entire length vertically. The process continues on the second row until all horizontal and vertical pixels go through a convolution process according to the pattern of the Canny kernel.

$$G=|G_x|+|G_y| \quad (14)$$

Furthermore, to determine the direction of the edge used (15) which is denoted $\theta$. It is resulted from invers of tan $(\frac{G_y}{G_x})$ which have value between 0 and 1. The value reconstruct a new image based on edge detection sharpened.

$$\theta=\arctan\left(\frac{G_y}{G_x}\right) \quad (15)$$

Then the process of eliminating non-maximum values (non-maxima suppression) is carried out. If the intensity value is not maximum, the pixel value will be decreased to 0. The next step is the thresholding process using the threshold values *T min* and *T max* as in (16). g(x) value determines the last result on binary value, 0 and 1. It is an edge of the image sharped. A number of the edge of images forms a feature map.

$$g(x,y)=\begin{cases} 1, \text{jika } T_{min} \le f(x,y) \le T_{max} \\ 0, \text{otherwise} \end{cases} = \quad (16)$$

**2.2.5. Proposed method: combination edge detection**

The combination technique is an approach that researchers take to obtain maximum feature extraction results. The technique is to combine the edge detection of Robert ($G_{x1}$), Prewitt ($G_{x2}$), Sobel ($G_{x3}$), and Canny ($G_{x4}$) based on (17) and (18). The pixel mapping for each image on each edge detection will be aggregated by row horizontally and vertically. The pixels shift process along the horizontal will be summed based on the Gx notation. While the vertical direction, the pixels shift process vertically is added to the total number of shifts, Gy notation.

$$G_x = G_{x1} + G_{x2} + G_{x3} + G_{x_4} \quad (17)$$

$$G_y = G_{y1} + G_{y2} + G_{y3} + G_{y4} \quad (18)$$

In (17) and (18) show the process of the sum of edge detections in the horizontal ($G_x$) and vertical ($G_y$) directions. Each edge detection will give each other a strengthening effect on the image object. If one edge detection gives a dark side at the edges, then the other edge detection will give a good effect, sharpening every edge of the face object. The sound effect on each edge would give a name to the outline of the eyebrows, eyes, nose, and mouth. This effect will provide a precise extraction in binary or numeric values to be continued in the classification and recognition process.

### 2.3. Classification using multi distance measure

#### 2.3.1. Euclidean distance

The Euclidean distance (ED) method compares the minimum distance of the test image with the training image database [12], [22]. The ED of the two vectors x and y is calculated by (19) [23]:

$$\mathrm{d}(x, y) = \left(\sum_i (x_i - y_i)^2\right)^{\frac{1}{2}} \quad (19)$$

The smaller the value of d(x, y), the more similar the two vectors are compared. On the other hand, the greater the value of d(x, y), the more different the two vectors are matched.

#### 2.3.2. Canberra distance

Canberra distance (CD) is used to get the distance from a pair of points where the data is original and in a vector space. CD provides output in the form of actual (true) and false (false) values as shown in (20) [23]–[25].

$$D_{x,y} = \sum_{k=1}^{n} \frac{|x - y|}{(x+y)} \quad (20)$$

$D_{xy}$ as CD process, $x$ as gallery image vector, $y$ as probe image vector, and $k$ as vector number.

#### 2.3.3. Mahalanobis distance

This distance is defined as the distance between two points involving a multiplier and can reduce distance distortion caused by linear combinations, as shown in (21) [26]. The Mahalanobis distance (MD)-based score is calculated as the minimum squared MD as shown in (21) [27].

$$D(x, y) = \sqrt{(x - y)^T C^{-1} (x - y)} \quad (21)$$

MD is obtained by calculating multiplication elements, both of transpose and inverse of covariance. Transpose and inverse of covariance to the difference between training data and testing data. MD will produce the square root of the product of both.

### 2.4. Performance measure

The performance testing indicates the proposed method results from the summation of the four edge detection vectors. Furthermore, the distance measure calculates the error between the training data and the testing data. The confusion matrix determines the validation between both data. It also determines whether a model performs better or worse. percentage of accuracy obtained from multi-edge detection and multi-classifier techniques.

The percentage of accuracy is the level of performance. The confusion matrix denotes the error rate in the vector form with a 2×2 matrix which deals with the four terms such as true positive signifies correctly identified, true negative, false positive, and false negative [22].

$$\text{Confusion Matrix} = \begin{bmatrix} True\ Negative\ (TN) & False\ Positive\ (FP) \\ False\ Negative\ (FN) & True\ Ppositive\ (TP) \end{bmatrix}$$

These measure can be constructed by metrics: (1) true positive is the number of valid classified of images gallery and faces probe; (2) true negative is the number of valid classified of outer images galley and faces probe [28], [29] as shown in (22).

$$\text{Accuracy} = \left(\frac{True\ Positive + True\ Negative}{Total\ number\ of\ images}\right) x\ 100\% \quad (22)$$

## 3. RESULTS AND DISCUSSION

### 3.1. Data acquisition

The data acquisition stage was resizing from the original size to a 100×100 image, and from a color image to a greyscale image as shown in Figure 2. Each pixel has an image component of red, green, and blue (RGB) as the primary component of the image color. This value went through a greyscale process that added up each color component value and then divided by 3. Its results were greyscaled images on a 0-255 scale as shown in Figure 2.

Each face image has five poses on position: straight front view; 15° right tilt view; 15° left tilt view. Facial expression and eyes sight are flexible, smile, flat, or free. The registered on the face is stored on face gallery or image database.

Figure 2. Image dataset in image gallery [30]

### 3.2. Face extractor using multi-edge detection

There were five stages of the edge detection process at the feature extraction stage. The detection techniques were Robert, Prewitt, Sobel, Canny, and Combination. They resulted in pixel value in 5×5 size (Figure 3). A 25 pixels image-shaped feature map based on the extraction pattern of multi-edge detection. Multi-edge detection had a mean of 116,333 pixels. The proposed method showed higher pixel value than others because it was the sum result of Robert, Prewitt, Sobel, and Canny. The feature map values were differentiators of an image and the others. They were so identity value of the person concerned when the training and testing were processing.

| | 0 | 1 | 2 | 3 | 4 | 5 | 6 | 7 | 8 | 9 | 10 | 11 | 12 | 13 | 14 | 15 | 16 | 17 | 18 | 19 | 20 | 21 | 22 | 23 | 24 |
|---|---|---|---|---|---|---|---|---|---|---|---|---|---|---|---|---|---|---|---|---|---|---|---|---|---|
| **Robert** | 87 | 93 | 39 | 91 | 205 | 137 | 43 | 32 | 90 | 255 | 177 | 37 | 39 | 139 | 255 | 160 | 17 | 13 | 106 | 255 | 255 | 251 | 255 | 255 | 144 |
| **Sobel** | 108 | 68 | 121 | 111 | 61 | 155 | 203 | 82 | 159 | 144 | 204 | 255 | 31 | 255 | 183 | 233 | 255 | 69 | 255 | 226 | 179 | 106 | 145 | 128 | 144 |
| **Prewitt** | 108 | 68 | 121 | 111 | 61 | 155 | 251 | 73 | 125 | 144 | 204 | 223 | 49 | 248 | 183 | 233 | 232 | 43 | 169 | 226 | 179 | 106 | 145 | 128 | 144 |
| **Canny** | 108 | 68 | 121 | 111 | 61 | 155 | 255 | 218 | 199 | 144 | 204 | 255 | 84 | 255 | 183 | 233 | 112 | 18 | 252 | 226 | 179 | 106 | 145 | 128 | 144 |
| **Combination** | 303 | 229 | 281 | 313 | 327 | 447 | 497 | 187 | 374 | 543 | 585 | 515 | 325 | 642 | 621 | 626 | 504 | 125 | 530 | 507 | 613 | 463 | 545 | 766 | 432 |

Figure 3. Feature map of 5×5 size image

Edge detections had different fluctuation values of a face image as Figure 4. The combination of adding convolution value of the four edge detections. Feature extraction had different values depending on the type used. The proposed method had a higher value because it had been the sum of the four feature extractions, Robert, Sobel, Prewitt, Canny, and Combination 1 and Combination 2 respectively. This value had not indicated accuracy, but it indicated as the lowest to the highest feature vector. Combination 1 represents the feature extraction value of the summation of the four edge detections. Combination 2 represents the results of Combination 1 thresholding on 255 level as the highest level of greyscale. Thresholding cuts the feature extraction values if its values are greater than 255 as 255.

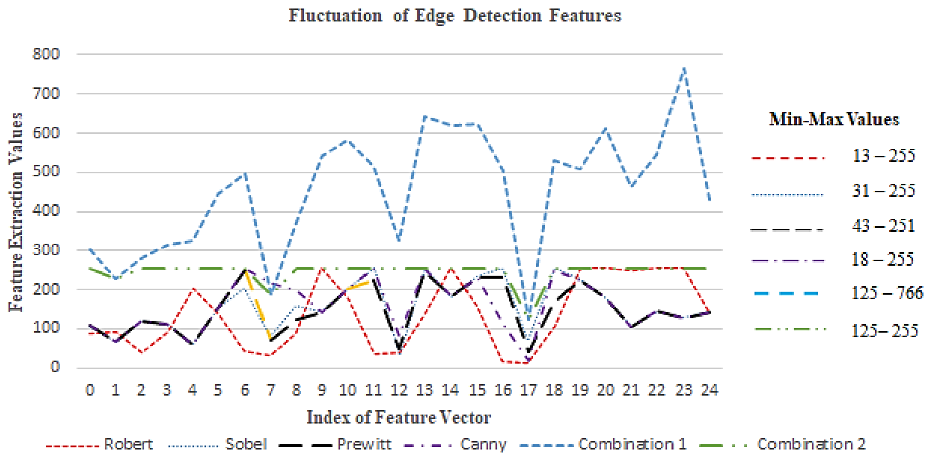


Figure 4. Fluctuation of multi edge detection

The feature extractions proposed have a visualization of edge detection such on Figure 5. They are i) Robert edge detection, ii) Prewitt edge detection, iii) Sobel edge detection, iv) Canny edge detection, and v) Combination edge detection. Robert edge detection has smoother and very thin gradations or contours on the eyebrows, eyes, nose, and mouth; visually, it is challenging to capture the object because some points are given contour reinforcement. Prewitt edge detection has edges that are very sharp with amplification at the boundaries of the face, eyebrows, eyeballs, and nose very clearly, except the mouth is contoured with slightly blurred lines. Sobel edge detection strengthens the thin but more straightforward outlines between the boundaries of the face, eyebrows, eyeballs, nose, and mouth so that the sketch of a human face is perfecter and visible, somewhat close to the photo negative. Furthermore, Canny edge detection has very bright line boundaries so the differences in the contours of the facial properties are not apparent, only the edges do not show the contour differences between the facial property boundaries, so the information that this is a human face is still blurry. The process of perfecting the results of multi-edge detection is found in combination. It combines the four other edge detection.

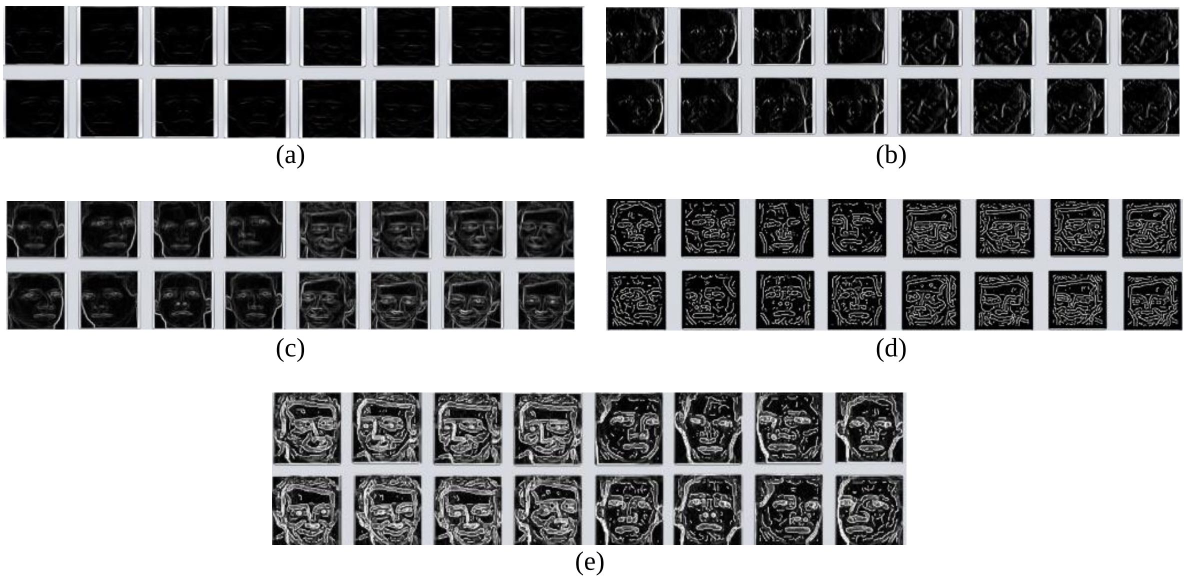


Figure 5. Visualization of multi edge detection. They are (a) Robert edge detection, (b) Prewitt edge detection, (c) Sobel edge detection, (d) Canny edge detection and (e) Combination edge detection [30]

It appears that the lines and contours of each facial property are prominent and bright at each edge. The light pixel value effect indicates it is less susceptible to noise than Sobel, who has fragile outlines even though a face's information is clear. Combination edge detection has advantages over the other four edge detections in terms of: outline, very clearly visible property boundaries of the face, eyebrows, eye curvature, eyeball, nose, and mouth; the contours, the area boundaries of each property, the height and the area, are very clearly visible so that if there is some blur or noise at some point, the facial properties will still be visible. The strengthening of these two lines, both the outline and the contour, provides an effective reinforcement to indicate the human face.

### 3.2. Classification using multi-distance measure

Distance measures determine the identity of the original face from the feature extraction in the cluster of dissimilarities between the training data and the testing data. If the value of the distance measure is getting smaller (if the distance≤0) then the performance is getting better, on the contrary, if the distance is getting bigger then the performance is getting worse.

Table 2 shows classification based on distance measure contains three classifiers that depend on feature extractors used. The classifiers outputs have a correlation with extractors. The face recognition process compares the value of the probe data (testing) with the face gallery, the value chosen as its identity is the smallest value of the distance measure. If the classification results show the same identity as the identity in the face gallery, then the data is said to be valid, otherwise, the data is said to be invalid.

The result of classifiers using the multi-classifier ED, CD, and MD shows that ED has 27 valid samples using Robert and combination edge detection; The CD has 100 valid samples using Sobel and Combination, and MD has 27 valid samples on Robert and Combination. It appears that the ED, CD, and MD have high invalid samples of 17 samples (Canny), 17 samples (Canny, respectively), and MD has 19 samples (Canny).

Table 2. The classification of distance measure

| Edge detection | Euclidean distance | | Canberra distance | | Mahalanobis distance | |
|---|---|---|---|---|---|---|
| | Valid | Invalid | Valid | Invalid | Valid | Invalid |
| Robert | 20 | 10 | 30 | 0 | 12 | 18 |
| Prewitt | 21 | 9 | 29 | 1 | 21 | 9 |
| Sobel | 26 | 4 | 30 | 0 | 25 | 5 |
| Canny | 13 | 17 | 13 | 17 | 11 | 19 |
| Combination | 27 | 3 | 30 | 0 | 27 | 3 |
| 5 | Canny | Combination | - | - | Canny | Combination |

Table 3 Rank of multi edge detection and multi classifier shows ED calculation results in the highest rank on combination edge detection and the lowest rank on Canny edge detection. The CD calculation results in the highest rank on Robert, Sobel, and Combination and the lowest rank on Canny. The validation between training data and testing data is based on the Confusion matrix as previously mentioned. The smallest distance value determines the face class or the authentic owner is the same as in the face gallery. The greater value indicates the more significant difference. The validation results obtained show that there are many values closeness between the gallery faces and the probe faces.

Table 3. Rank of multi edge detection and multi classifier

| Rank | Euclidean distance | | Canberra distance | | Mahalanobis distance | |
|---|---|---|---|---|---|---|
| | True | False | True | False | True | False |
| 1 | Combination | Canny | Robert, Sobel, Combination | Canny | Combination | Canny |
| 2 | Sobel | Robert | Prewitt | Prewitt | Sobel | Robert |
| 3 | Prewitt | Prewitt | Canny | Robert, Sobel, Combination | Prewitt | Prewitt |
| 4 | Robert | Sobel | - | - | Robert | Sobel |

### 3.3. Performance measure

Performance measurement uses an accuracy calculation based on the genuine acceptance rate (GAR) and FAR. GAR indicates the level of excellence of the proposed method. On the other hand, FAR indicates the level of weakness. The advantages and disadvantages refer to the level of recognition. The higher the GAR value, the better the system accuracy, and vice versa. In contrast to FAR, the lower the FAR, the better the performance of the proposed method, and the higher the value, the lower the performance in Table 4. Figure 6 results of distance measure regression indicate metrics in Figure 6(a) GAR standard deviation of distance measure and Figure 6(b) FAR standard deviation of distance measure.

Table 4. The Recognition result of proposed method

| Distance measure | GAR mean | GAR standard deviation | FAR mean | FAR standard deviation |
|---|---|---|---|---|
| Euclidean distance | 11,505.780 | 1,425.258 | 13,447 | 536.472 |
| Mahalanobis distance | 11,008.260 | 1,133.066 | 12,672 | 787.629 |
| Canberra distance | 3,882.133 | 294.965 | 0 | 0 |

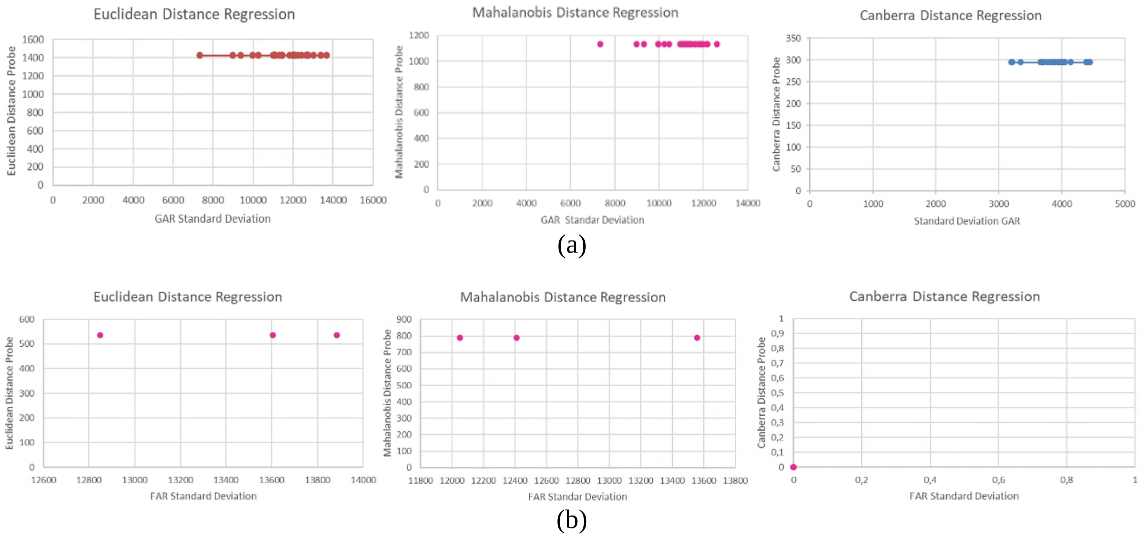


Figure 6. Results of distance measure regression (a) GAR standard deviation of distance measure and (b) FAR standard deviation of distance measure

The CD GAR has a lower standard deviation so its accuracy outperforms other distance measures (Figure 6). The CD has a 0 FAR value because it does not have an invalid test image. Comparing the standard deviation (Figure 6) of classifiers results to distinguish between authentic face image and an-authentic face image. The standard deviation shows the small till the high standard deviation in i) GAR standard deviations is small (Euclidean distance), middle (Mahalanobis distance), and high (Canberra distance); and ii) FAR standard deviation are small (Euclidean distance), middle (Mahalanobis distance), and high (Canberra distance). If the classifier has the a smaller standard deviation than other classifiers, then GAR and FAR are better. Otherwise, if the classifier has a standard deviation higher than others, then GAR and FAR are worst. The better performance of GAR and FAR is Canberra Distance. It has a significant distinguishing element.

Tabel 5 shows the performance of feature extraction and classifier (%). The percentage value had gotten confusion matrix validation. The value is different for each feature extraction and classifier. feature type and classification determine the best performance. The best performance on feature extraction is the combination outperforms the four others. Likewise, the best classifier in Canberra distance outperforms ED and MD.

Table 5. The performance measures

| Edge detection | Distance measure | | |
|---|---|---|---|
| | Euclidean distance | Canberra distance | Mahalanobis distance |
| Robert | 66.67% | 100.00% | 40.00% |
| Prewitt | 70.00% | 96.66% | 70.00% |
| Sobel | 86.66% | 100.00% | 83.33% |
| Canny | 43.33% | 43.33% | 36.66% |
| Combination | 90.00% | 100.00% | 90.00% |

Figure 7 describes comparing the performance of multi-edge detection and distance measure in two categories. There are five color curves, Sobel, Prewitt, Robert, and Canny, respectively: (a) true positive; on the other hand; and (b) false negative, the highest false negatives are Canny, Robert, Prewitt, Sobel, and Combination. The combination edge detection has the highest accuracy in face recognition compared to the other four methods, as shown by each color of the line indicator. Every additional data has a better accuracy suitable for the increasing number of training data and testing data provided.

The proposed method result has the best performance by 90.00% at ED, 100% at CD, and 90% at MD. The results outperform [9], [15]–[20], [22], [23] using two or more feature extractors, both edge detection and others. The combination edge detection has good performance equals research results conducted by [14], [23]–[25].

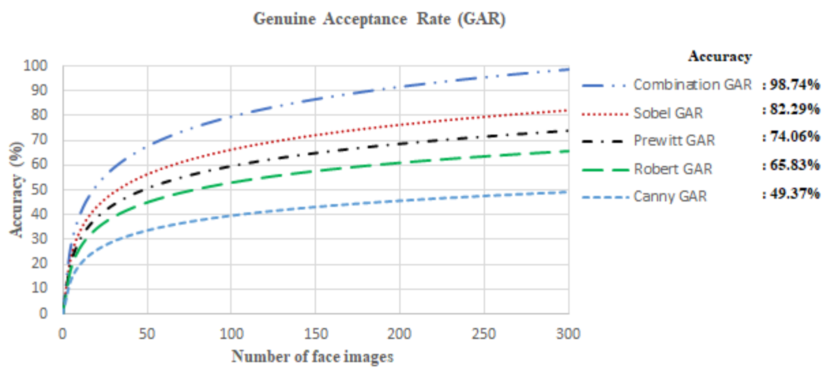


(a)

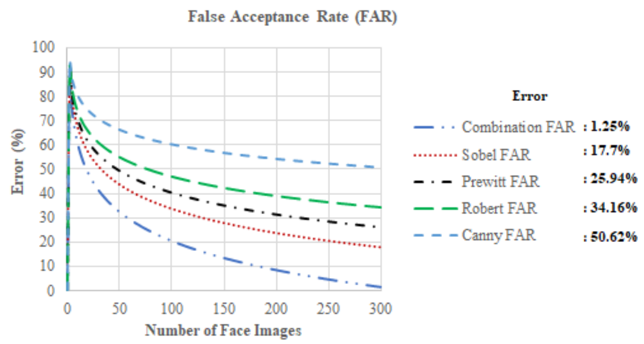


(b)

Figure 7. The performance of multi edge detection and distance measure: (a) true positiveand (b) false positive

The proposed method performance outperforms the other four detections. It has the highest GAR. Otherwise, it has the lowest FAR. The trends showed a quite significant result than the previous research. Optimizing edge detection means providing a border pattern line representing a person's face image. The solution is to use a multi-layer feature extractor to provide optimal feature extraction results to solve this problem. The following process is through classification using a multi-distance measure which has a matching process between the probe face and the face gallery. Distance measure shows the best accuracy is given by the edge detection combined with a significant difference compared to the other four feature extraction techniques. This proves that using multiple edge detection will reduce noise and distortion in the face image object. The initial stages will be optimal for the advanced processing stages of the face recognition system.

## 4. CONCLUSION

Combination edge detection provides the best performance among multi-edge detection. Comparing all edge detection classifier methods indicates that the combination edge detection contributes to a unique extraction value because it reduces noise and provides contour reinforcement to facial properties. This method can be used in developing facial recognition applications. The performance of the combination edge detection and classifier Canberra distance has a stable performance to be applied to facial recognition systems that use specifications of limited memory capacity and device speed that is not too high. Further development for researchers at the feature extraction stage is recommended to use combination edge detection as face detection quickly. Next, verify and identify faces using other more detailed methods to vector accurately analyze facial properties. It will provide a proportional facial biometric performance that accommodates human needs to develop the latest human civilization.

**ACKNOWLEDGEMENTS**

We say we thank the Rector of Universitas Dipa Makassar for the support in the form of motivation, encouragement, and funding for this research publication.

## REFERENCES

[1] M. Jovic, S. M. Cisar, and P. Cisar, "Delphi application for face detection using the sobel operator," in *CINTI 2012 - 13th IEEE International Symposium on Computational Intelligence and Informatics, Proceedings*, 2012, pp. 371–376, doi: 10.1109/CINTI.2012.6496791.

[2] C. I. Gonzalez, P. Melin, J. R. Castro, O. Mendoza, and O. Castillo, "An improved sobel edge detection method based on generalized type-2 fuzzy logic," *Soft Computing*, vol. 20, no. 2, pp. 773–784, 2016, doi: 10.1007/s00500-014-1541-0.

[3] Z. E. M. Osman, F. A. Hussin, and N. B. Z. Ali, "Hardware implementation of an optimized processor architecture for SOBEL image edge detection operator," in *2010 International Conference on Intelligent and Advanced Systems, ICIAS 2010*, 2010, no. 1, pp. 2–5, doi: 10.1109/ICIAS.2010.5716147.

[4] P. Ganesan, V. Rajini, and R. I. Rajkumar, "Segmentation and edge detection of color images using CIELAB Color Space and Edge detectors," in *International Conference on "Emerging Trends in Robotics and Communication Technologies", INTERACT-2010*, 2010, pp. 393–397, doi: 10.1109/INTERACT.2010.5706186.

[5] S. Das, "Comparison of various edge detection techniques," in *2015 International Conference on Computing for Sustainable Global Development, INDIACom 2015*, 2015, pp. 393–396, doi: 10.14257/ijsip.2016.9.2.13.

[6] J. Liu and Y. Huang, "Study of human face image edge detection based on DM642," in *2010 3rd International Conference on Computer Science and Information Technology*, 2014, vol. 8, pp. 175–179, doi: 10.1109/ICCSIT.2010.5563574.

[7] W. Gao, L. Yang, X. Zhang, and H. Liu, "An improved Sobel edge detection," in *Proceedings - 2010 3rd IEEE International Conference on Computer Science and Information Technology, ICCSIT 2010*, 2010, vol. 5, pp. 67–71, doi: 10.1109/ICCSIT.2010.5563693.

[8] S. Liu, X. Tang, and D. Wang, "Facial expression recognition based on sobel operator and improved CNN-SVM," in *2020 3rd IEEE International Conference on Information Communication and Signal Processing, ICICSP 2020*, 2020, pp. 236–240, doi: 10.1109/ICICSP50920.2020.9232063.

[9] H. C. V. Lakshmi and S. Patilkulakarni, "Segmentation algorithm for multiple face detection for color images with skin tone regions," in *2010 International Conference on Signal Acquisition and Processing, ICSAP 2010*, 2010, pp. 162–166, doi: 10.1109/ICSAP.2010.42.

[10] Y. Ramadevi, T. Sridevi, B. Poornima, and B. Kalyani, "Segmentation and object recognition using edge detection techniques," *International Journal of Computer Science and Information Technology*, vol. 2, no. 6, pp. 153–161, 2010, doi: 10.5121/ijcsit.2010.2614.

[11] Y. Kortli, M. Jridi, A. Al Falou, and M. Atri, "A novel face detection approach using local binary pattern histogram and support vector machine," *2018 International Conference on Advanced Systems and Electric Technologies, IC_ASET 2018*, no. March, pp. 28–33, 2018, doi: 10.1109/ASET.2018.8379829.

[12] F. Smach, J. Miteran, M. Atri, J. Dubois, M. Abid, and J. P. Gauthier, "An FPGA-based accelerator for fourier descriptors computing for color object recognition using SVM," *Journal of Real-Time Image Processing*, vol. 2, no. 4, pp. 249–258, 2007, doi: 10.1007/s11554-007-0065-6.

[13] I. Intan, "Combining of feature extraction for real-time facial authentication system," in *2017 5th International Conference on Cyber and IT Service Management, CITSM 2017*, 2017, pp. 1–6, doi: 10.1109/CITSM.2017.8089223.

[14] N. Boyko, O. Basystiuk, and N. Shakhovska, "Performance evaluation and comparison of software for face recognition, based on Dlib and Opencv library," in *Proceedings of the 2018 IEEE 2nd International Conference on Data Stream Mining and Processing, DSMP 2018*, 2018, pp. 478–482, doi: 10.1109/DSMP.2018.8478556.

[15] A. Noori Hashim and N. Kream Shalan, "Face recognition using hybrid techniques," *Journal of Engineering and Applied Sciences*, vol. 14, no. 12, pp. 4158–4163, 2019, doi: 10.36478/jeasci.2019.4158.4163.

[16] S. H.KrishnaVeni, K. L. Shunmuganathan, and L. Padma Suresh, "A Novel NSCT based illuminant invariant extraction with optimized odge detection technique for face recognition," *International Journal of Computer Applications*, vol. 70, no. 3, pp. 7–10, 2013, doi: 10.5120/11940-7733.

[17] M. R. Faraji and X. Qi, "Face recognition under illumination variations based on eight local directional patterns," *IET Biometrics*, vol. 4, no. 1, pp. 10–17, Mar. 2015, doi: 10.1049/iet-bmt.2014.0033.

[18] A. S. O. Ali, V. Sagayan, A. M. Saeed, H. Ameen, and A. Aziz, "Age-invariant face recognition system using combined shape and texture features," *IET Biometrics*, vol. 4, no. 2, pp. 98–115, 2015, doi: 10.1049/iet-bmt.2014.0018.

[19] N. Kihal, S. Chitroub, A. Polette, I. Brunette, and J. Meunier, "Efficient multimodal ocular biometric system for person authentication based on iris texture and corneal shape," *IET Biometrics*, vol. 6, no. 6, pp. 379–386, Nov. 2017, doi: 10.1049/iet-bmt.2016.0067.

[20] D. Manju and V. Radha, "A novel approach for pose invariant face recognition in surveillance videos," *Procedia Computer Science*, vol. 167, no. 2019, pp. 890–899, 2020, doi: 10.1016/j.procs.2020.03.428.

[21] X. Chen and W. Cheng, "Facial expression recognition based on edge detection," *International Journal of Computer Science & Engineering Survey*, vol. 6, no. 2, pp. 1–9, Apr. 2015, doi: 10.5121/ijcses.2015.6201.

[22] M. Razzok, A. Badri, I. El Mourabit, Y. Ruichek, and A. Sahel, "A new pedestrian recognition system based on edge detection and different census transform features under weather conditions," *IAES International Journal of Artificial Intelligence (IJ-AI)*, vol. 11, no. 2, pp. 582–592, Jun. 2022, doi: 10.11591/ijai.v11.i2.pp582-592.

[23] Y. Sari, M. Alkaff, and R. A. Pramunendar, "Iris recognition based on distance similarity and PCA," in *AIP Conference Proceedings*, 2018, vol. 1977, no. June, p. 020044, doi: 10.1063/1.5042900.

[24] R. Vashistha and S. Nagar, "An intelligent system for clustering using hybridization of distance function in learning vector quantization algorithm," in *2017 Second International Conference on Electrical, Computer and Communication Technologies (ICECCT)*, Feb. 2017, pp. 1–7, doi: 10.1109/ICECCT.2017.8117856.

[25] D. González-Jiménez *et al.*, "Distance measures for Gabor jets-based face authentication: a comparative evaluation," *Lecture Notes in Computer Science (including subseries Lecture Notes in Artificial Intelligence and Lecture Notes in Bioinformatics)*, vol.

4642 LNCS, pp. 474–483, 2007, doi: 10.1007/978-3-540-74549-5_50.
[26] Y. Wang, G. Nie, N. Hu, and B. Chen, "Bearing health assessment based on different types of masses voting match and Mahalanobis mistance under different operating conditions," in *Proceedings of the 2nd International Conference on Artificial Intelligence and Advanced Manufacture*, Oct. 2020, pp. 340–343, doi: 10.1145/3421766.3421870.
[27] R. Kamoi and K. Kobayashi, "Why is the Mahalanobis distance effective for anomaly detection?," *arXiv preprint arXiv:2003.00402*, Feb. 2020, doi: 10.48550/arXiv.2003.00402.
[28] H. A. Abu Alfeilat *et al.*, "Effects of distance measure choice on K-nearest neighbor classifier performance: a review," *Big Data*, vol. 7, no. 4, pp. 221–248, 2019, doi: 10.1089/big.2018.0175.
[29] A. Pillai, R. Soundrapandiyan, S. Satapathy, S. C. Satapathy, K. H. Jung, and R. Krishnan, "Local diagonal extrema number pattern: a new feature descriptor for face recognition," *Future Generation Computer Systems*, vol. 81, no. November, pp. 297–306, 2018, doi: 10.1016/j.future.2017.09.055.
[30] M. Tavares, "The ORL database for training and testing," *Kaggle.Com*, 2020. https://www.kaggle.com/tavarez/the-orl-database-for-training-and-testing/is accessed 2021 May 4th.

## BIOGRAPHIES OF AUTHORS

**Indo Intan** holds a Bachelor of Engineering (S.T.) in Electrical Engineering, a Master of Computer, Control, and Electronic Engineering from Hasanuddin University, Makassar, Indonesia in 2010, with the Thesis "Pattern Recognition of Thyroid Carcinoma Hystophatologic using ANFIS". He is currently lecturing with the department of Informatics Engineering at Universitas Dipa Makassar, Makassar, Indonesia. Her research interests are in image processing, pattern recognition, machine learning and internet of thing. She can be contacted at email: indo.intan@undipa.ac.id.

**Nurdin** earned a Bachelor's degree in Computer Science at STMIK Dipanegara Makassar, Indonesia in 1999. He earned a Master's degree in Engineering from Hasanuddin University, Indonesia in 2007. He is currently a lecturer in the Department of Informatics Engineering at Dipa University Makassar. His research includes computer security, network security, cyber security, machine learning, and data mining. He can be contacted at email: nurdin@undipa.ac.id.

**Fitriaty Pangerang** earned a Bachelor's degree in at electrical engineering Hasanuddin University in 1997. She He earned a Master's degree in Engineering from Hasanuddin University, Indonesia in 2007. She is currently a lecturer in the Department of Electronics Engineering at Polytechnic Negeri Ujung Pandang. She researches electronic control, electronic instrumentation, and electronic digital system. She can be contacted at email: fpangerang@gmail.com.